Adaptive Asymmetric Linearization of Radio Over Fiber Links for Wireless Access

Xavier N. Fernando, *Member, IEEE,* and Abu B. Sesay, *Senior Member, IEEE*

***Abstract*—The biggest concern in the use of radio-over-fiber (ROF) links in wireless access is their limited dynamic range due to nonlinear distortion (NLD). In this paper, a higher order adaptive filter based nonlinearity compensation scheme is proposed. Pre-compensation is done for the downlink while post-compensation is done for the uplink to result in asymmetry with respect to complexity. This centralized signal processing is attractive in that it keeps the remote unit simple. Accurate measurements of ROF link parameters are not required with this approach because the filters are adapted from the distortion of the input/output base band signal. This technique also facilitates fast tracking of modifications and drifts in the link characteristics. Measurements and simulation results show that gradually saturating amplitude nonlinearity can be adequately linearized with some backoff from the clipping limit. A 42% backoff is required for pre-compensation to protect the laser while only a 16.7% backoff is required for post-compensation. Phase pre-compensation is accomplished with a higher accuracy than phase post-compensation.**

***Index Terms*—Adaptive filters, communication system nonlinearities, compensation, land mobile cellular radio systems, nonlinear distortion, optical fiber communication.**

I. Introduction

TO MEET the explosive demands of high-capacity and wide-band access, personal communication system (PCS) applications, it becomes necessary to split existing cells into micro-cells and pico-cells. In a conventional system, it would be required to deploy a base station in each micro-cell and pico-cell, which is too costly because of the very large number that is required. In this paper, a more economical approach, which combines a wireless link and an optical fiber link, is proposed. In this proposal, after a cell is split, a single central base station is deployed to serve a group of micro-cells or pico-cells. A radio access point (RAP) is placed in each micro-cell or pico-cell to provide wireless access to the portables and is linked to the central base station via optical fiber as shown in Fig. 1. For the downlink transmission, data is first processed and converted into an optical signal for transmission over the fiber link to the RAP. At the RAP, the optical signal is converted into an RF signal, which is amplified and relayed to the portables via wireless channels. In the uplink, operations are performed in the reverse order. The basic components of the RAP include an optical-to-electrical (O/E) converter, an electrical-to-optical (E/O) converter for downlink and uplink, respectively, and a radio antenna as well as an RF amplifier. The RF amplifier is needed to compensate power loss in the optical as well as the wireless link. The RAP is signal format independent so that a single physical layer can support multiple services. Most of the signal processing such as up/down conversion, modulation/demodulation, equalization, error correction, is done at the central base station (where cost is shared by many users) and at the portable. This helps reduce deployment cost, power consumptions and maintenance requirements.

The radio-over-fiber (ROF) or optical link portion of the system usually has adequate bandwidth to support wide-band and high capacity services. However, when the wireless link is in series with the ROF link, especially in a multi-user environment, nonlinear distortion (NLD) of the ROF link, due mainly to the laser diode, becomes the biggest concern. The high-gain RF amplifier may also introduce additional nonlinear distortion. Furthermore, the dynamic range (distortion-free range for the input signal) is severely reduced as a result of path loss, fading, and shadowing in the wireless link. The dynamic range requirement of the uplink in a typical microcellular environment is in the range of 80–90 dB [1]. On the other hand, the dynamic range available from a typical ROF link is about 20–30 dB less than the above requirement. Also, the varying number of users and high peak-to-average ratios of the signal envelope combined with forward-loop power control schemes demand large dynamic range. In order to meet the large dynamic range demand, the nonlinearity introduced by the laser diode and the RF amplifier must therefore be compensated.

A. Previous Work

Several approaches have been proposed to characterize and solve the problem of NLD [1]–[12]. These approaches can be grouped into three major categories. The first category attempts to directly model the laser by either solving the laser rate equations or by using equivalent circuit models as in [2] and [3]. The "post nonlinearity recovery block" in [4] and electronic pre-distortion schemes in [5] and [6] extend this approach to inverse model the laser. The solution would be accurate if the physical parameters of the device were accurately known. However, apart from not usually being available, these parameters are device dependent. For example, large differences have been reported [17] in the modulation response of similar distributed feedback lasers. In addition, other unknown nonlinear elements in the link may also have to be adequately modeled if this approach is used.

The second category suggests compressing the signal within the linear range of the ROF link. Automatic gain controllers and the automatic attenuation technique of [8] fall under this category. However, because of the variations in the timing of stimu-

Manuscript received January 8, 2001; revised November 27, 2001; accepted April 2, 2002. This work was supported by TRLabs and Natural Science and Engineering Research Council (NSERC) of Canada.

X. N. Fernando is with Ryerson University, Toronto, ON M5B 2K3, Canada.
A. B. Sesay is with University of Calgary, Calgary, AB T2N 1N4, Canada.

Digital Object Identifier 10.1109/TVT.2002.804841

lated photon generation, even in the so-called linear region, the phase response of the laser is nonlinear. The approach does not address this issue and also demands additional (linear) amplification at the receiver.

Some authors have proposed to mitigate the NLD in the network layer. One way is to allocate frequency channels to the ROF link in a way such that the cross-modulation products do not overlap [1]. However, this will reduce trunking capacity. Another proposal is to use more than one RAP per micro-cell in [9] (RAP diversity), however, this would significantly increase infrastructure cost. Another work [10] suggests to cancel the NLD in the same way as multi-user interference is canceled in code division multiple access (CDMA) schemes. This, however, would further increase the complexity of already complex CDMA receivers. Furthermore, none of these techniques solves the emission problem.

B. Proposed Approach

Rather than focus on the internal electronics and the modeling of the element by element contribution, we focus on the composite effect of the nonlinear distortions. This may be done by investigating the input–output characteristic of the nonlinearity. We first conduct experimental measurements on a typical link to characterize the composite nonlinearity. We then propose a model that best matches the measured characteristics. Knowing the model of the mechanism that generates the nonlinearity, we propose adaptive signal processing algorithms to generate the inverse model, which when placed in cascade, will eliminate the nonlinearity. In this paper, a higher order adaptive filter based compensation scheme is proposed and described for the entire ROF link including all cascaded nonlinearities. When a photonic device is replaced, it is only necessary to adapt the filter parameters to match the input–output characteristics during a training period. This matching is accomplished through adaptive signal processing. We have proposed a phase pre-distortion scheme in [13] and a post-compensation scheme in [14] separately. Phase compensation is required because the data information of interest is contained in both the amplitude and the phase. A combined asymmetrical compensation of the amplitude and phase for both the uplink and the downlink is proposed in this paper. Major issues of this asymmetrical configuration are also discussed.

The amplitude and phase distortions of vector-modulated symbols are compensated with four separate filters. Two filters (one for phase and one for amplitude) are used in the downlink and two filters in the uplink. The filters adaptively train themselves from the distorted symbols so that no accurate knowledge of the laser diode and the physical link parameters is required. No RF/photonic circuit design is involved since the filters run at base band. The recursive least squares (RLS) algorithm is used for the adaptation. Any modification, replacement of laser diodes or drift in the link parameters are easily tracked by the algorithm. To obtain the asymmetrical compensation scheme, all the filters are placed at the central base station. This enables cost sharing between base station and RAP. RF emission requirements in the down link are not violated because the compensation is done before the wireless transmission.

The paper is organized as follows. Section II describes a micro-cellular wireless network and the role of the ROF link in the system. Section III discusses each element of the ROF in order to provide a better understanding of the sources, the nature of the nonlinearity and justification of our proposal. Section IV provides a mathematical background on Volterra type adaptive filters and describes how the filters are configured to compensate for the ROF link nonlinearity. Section V describes the hardware, measurements, and simulation results. Section VI concludes the paper and discusses the significance and limitations of these results in a practical system.

II. System Overview

The system under consideration is a micro-cellular/pico-cellular network. Each micro-cell or pico-cell consists of several wireless portables and a RAP. One base station serves several RAPs. Each RAP is connected to a central base station via two radio over fiber (ROF) links—the uplink and the downlink. The portables can transmit and receive voice, data, or video over the wireless channel depending on the application. This type of system has wide applications, for example, wireless-data and video communication (LAN type) services are in high demand for indoors. Furthermore, wireless voice communication in the office is very attractive since cordless PBX systems allow high degree of mobility. With the proposed arrangement, the wireless link is short and often a line-of-sight path is available so that high-speed services are easily accommodated. Furthermore, crowded places like campus premises and downtown offices can be configured into cost-effective micro-cells/pico-cells. This is also useful for hard to reach areas like tunnel zones where conventional cellular wireless signals would not normally reach.

A. Link Description

The system block diagram is shown in Fig. 1 for a single micro-cell and a single portable. In the uplink, the RAP receives a wireless (RF) signal from the portable unit and amplifies it. The amplified RF signal, after dc shifting, intensity modulates the laser (E/O) and generates a radio frequency optical signal in the fiber. At the other end of the fiber, the optical receiver, located in the central base station, detects the radio signal (O/E). This signal is then band pass filtered, amplified and demodulated to base band where the post-compensation filter corrects NLD. Because of the dc shifting, intensity modulation and direct detection do not remove the phase contained in the original RF signal. However, phase errors due to the NLD will be added to the original phase.

In the downlink, complex base-band symbols emanating from the central base station are appropriately pre-distorted by the pre-compensation filters before RF modulation. The RF signal, after dc shifting, intensity modulates the laser for transmission through the fiber. At the other end of the fiber, which is in the RAP, direct detection is accomplished to recover the original RF signal. The RF signal, with its phase preserved, is amplified and then radiated into the wireless channel. As noted above, the detected RF signal will contain the original phase as well as phase errors due to the NLD.

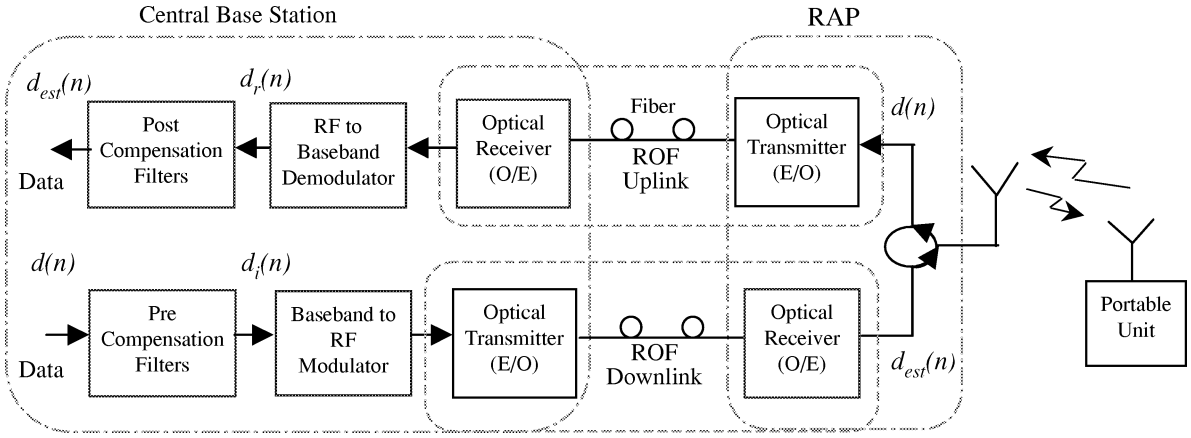

Fig. 1. Optical wireless access with asymmetric compensation.

The RAP acts as a wireless receiver as well as an optical transmitter in the uplink. In the downlink, it acts the other way round. In addition, more amplification is required in the downlink than in the uplink due to wireless transmission requirements. A suitable frequency or time duplexing scheme is assumed. This and other, not so relevant system issues are not discussed here.

III. Radio Over Fiber Link

In this section, we discuss the major elements of a directly modulated ROF link in order to provide a better understanding of the nonlinearity and to explain why the conventional compensation schemes would not work in this application. Direct modulation is considered here since it is the most cost effective and robust solution when the RF signal is within a few gigahertz. The application of interest in this paper is the PCS band around 1.9 GHz.

A. Laser Diode Transmitter

Stimulated and spontaneous emission mechanisms combined with gain compression characteristics make the laser inherently nonlinear. Semiconductor laser nonlinearity has been categorized into static and dynamic nonlinearity [11]. Static nonlinearity is frequently described with a third order polynomial. The laser output optical power $P_{\rm opt}(t)$ is a nonlinear function of the input electrical signal $s(t)$. The relation is shown in (1) for a third-order nonlinearity, where "m" is the optical modulation index, A_2 and A_3 are device dependent nonlinearity coefficients

$$P_{\rm opt}(t) = P_0\left[1 + ms(t) + A_2 m^2 s^2(t) + A_3 m^3 s^3(t)\right]. \quad (1)$$

The dynamic nonlinearity of the laser is described by well-known laser rate equations. In general, the dynamic nonlinearity is frequency dependent, however, if the modulating frequency is at least five times less than the laser resonance frequency it can be assumed to be frequency independent [11]. Although the dynamic nonlinearity would play an important role under transient conditions, it is not of major concern in data communications because only steady states conditions are of interest. It is the static nonlinearity of more concern.

In addition to the above, leakage current, and "axial hole burning" contribute to laser nonlinearity [15]. The leakage current nonlinearly increases with the injected current. "Axial hole burning" refers to the effect created when the optical power density along the length of the laser chip is nonuniform. This is especially noticeable with distributed feedback structures. All the above mentioned factors make direct modeling of a laser very difficult and inaccurate. Our proposal of modeling the input–output characteristics and adaptively compensating the composite nonlinearity is more attractive.

B. Single-Mode Fiber

Attenuation and chromatic dispersion are the two major concerns with a single-mode fiber. The attenuation is typically 0.5 dB/kM. The transfer function of the fiber reflecting the chromatic dispersion, as defined by CCITT, is given in (2), where "α" is a dispersion coefficient, l is the fiber length, $f - f_0$ is the radio frequency, and f_0 is the optical carrier frequency. Quantitative analysis using (2) shows that the chromatic dispersion is insignificant at PCS (1.9 GHz) frequencies up to several hundreds of kilometers of fiber length when the wavelength is 1310 nm. However, when the radio frequency is much higher and fiber is too long, fiber dispersion has to be considered, especially at 1550 nm. This is not a concern here, because the application of interest focuses around 1.9 GHz with a wavelength of 1310 nm and a fiber length of at most a few kilometers

$$H(f) = e^{-j\alpha l(f-f_0)^2}. \quad (2)$$

The directly modulated laser usually exhibits an unwanted frequency modulation called chirp that is typically around 150 MHz/mA. Although dispersive fiber would amplitude modulate chirp signals its effect is, however, negligible at a wavelength of 1310 nm with the short fiber length, which is of interest indoors at PCS frequencies. We have also experimentally confirmed this assumption.

C. Diode Receiver and Amplifier

Usually, faster photodiodes have smaller photosensitive areas to reduce inherent junction capacitance. These have relatively lower responsivity and may saturate at higher optical power. Nevertheless, in directly modulated links, the instantaneous optical power is limited by the laser nonlinearity and the detector usually operates within the linear region.

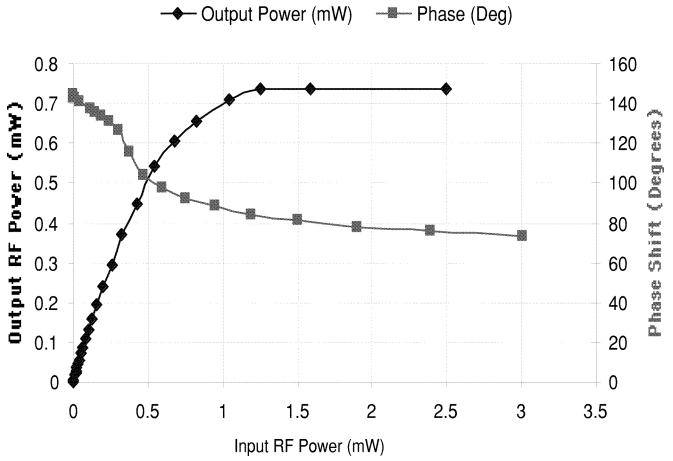

Fig. 2. Amplitude and phase response of the ROF link.

In a resistively matched, directly modulated ROF link about 30-dB loss is incurred due to O/E and E/O conversion alone [14]. Low conversion efficiency of the laser (0.1–0.15 mW/mA) is the major cause for this. In addition, fiber and connector losses would appear twice in the electrical domain. Reactive matching techniques decrease this loss, but they narrow down the useful bandwidth. Furthermore, the radio signal at the laser input has to be kept low to avoid extensive nonlinear distortion. Typical modulation depths are in the range of 10%–30%.

In general, because of the above factors, the radio signal level would be extremely low at the receiver. High-gain amplifier stages have to follow the detector, especially in the downlink to compensate the power loss. This amplifier would introduce additional nonlinear distortion (NLD). Linearity is always an issue with radio amplifiers. RF amplifier linearization is a big issue and extensive research is being done in that area [16], [17].

D. Experimental Measurements

Measured (experimental) responses of a typical ROF link are shown in Fig. 2, where the output RF power from the optical receiver is plotted versus the input RF power into the laser. These responses clearly show amplitude dependent amplitude (AM-AM) and amplitude dependent phase (AM–PM) distortions. The amplitude response linearly increases at first and then saturates. On the other hand, the phase response is quite nonlinear from the origin. This would severely impair the performance of a phase-modulated scheme.

In wireless systems, the number of users dynamically changes and the amplitude of each user signal varies due to fading. Furthermore, each subcarrier is distorted as a function of the total RF power through the link. This makes the solution extremely difficult, especially with conventional compensation methods which tend to be fixed solutions.

IV. Signal Processing

Whenever there is a requirement to process signals in an unknown environment, the use of adaptive filters offer a significant improvement over fixed filter solutions. Adaptive compensation is preferred here because numerous unknown parameters are involved.

In wireless communications, all the information is transmitted via vector-modulated symbols. A vector-modulated symbol is completely described by its phase and amplitude. Thus, all the ROF link impairment would ultimately contribute to phase and amplitude distortions of these symbols in addition to additive noise. By correcting these distortions, the ROF link can be effectively linearized. This is the fundamental justification behind the adaptive compensation approach.

The ROF link is a band-pass system. However, when the transmission is strictly band-limited, the nonlinear distortions introduced by band-pass nonlinearity can be completely described by a base-band memoryless nonlinearity [17]. This is further justified here because the NLD of ROF link is found to be frequency independent within the passband. Thus, for analysis and simulation we have considered a base-band equivalent for the entire system.

A. Volterra Series Adaptive Filters

The ROF link exhibits mild nonlinearity as a function of input RF power under steady-state conditions (Fig. 2). Therefore, it can be adequately modeled with a Volterra series filter. The output $d_1(n)$ of such a causal discrete-time, nonlinear system with input $p_1(n)$ is given by

$$d_1(n) = h_0 + \sum_{m_1=0}^{M} h_1(m_1)p_1(n-m_1) + \sum_{m_1=0}^{M}\sum_{m_2=0}^{M} h_2(m_1,m_2)p_1(n-m_1)p_1(n-m_2) + \cdots \quad (3)$$

In (3), $h_k(\ldots)$ is known as the kth-order Volterra kernel and M is the memory of the system. Usually, only the first few higher order terms in (3) are significant.

For nonlinearity compensation, the ROF link is inverse modeled with an adaptive filter that corresponds to another Volterra series filter. After convergence, the tap weights of this filter would formulate a higher order function, which is the inverse of the original function. This inverse filter is then placed in cascade to undo the nonlinear distortion. The expression for the inverse Volterra series filter output $d_2(n)$ is written as in (4), where $w_k(\cdot)$ is the kth tap weight and $p_2(n)$ is the input to the filter

$$d_2(n) = w_0 + \sum_{m_1=0}^{M} w_1(m_1)p_1(n-m_1) + \sum_{m_1=0}^{M}\sum_{m_2=0}^{M} w_2(m_1,m_2)p_2(n-m_1)p_2(n-m_2) + \cdots. \quad (4)$$

For efficient computation by adaptive algorithms, the weights $w_k(\cdot)$, $k = 0, 1, \ldots, N$ can be stacked into a vector $\mathbf{w}(n)$ as in

$$\mathbf{w}(n) = [w_0(n) \quad w_1(n) \quad \ldots \quad w_N(n)]^T. \quad (5)$$

The objective of the adaptive algorithm is to update the weight vector $\mathbf{w}(n)$ on a sample by sample basis so that the estimation error $e(n) = d(n) - d_{\text{est}}(n)$ between the desired output

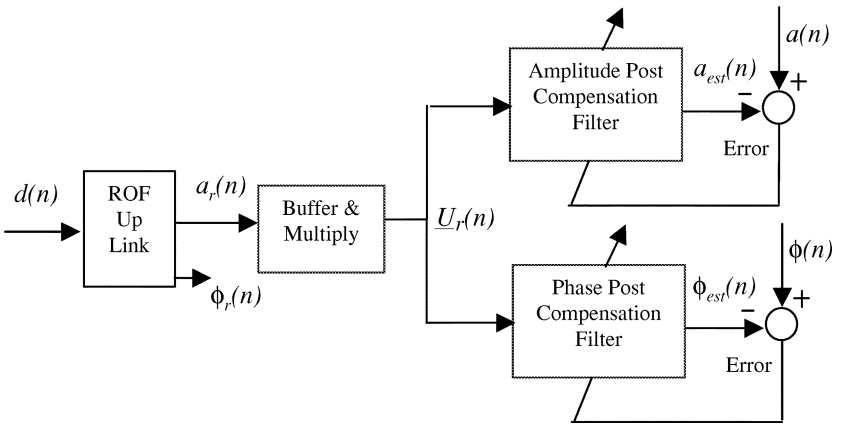

Fig. 3. Training arrangement for the post-compensation filter.

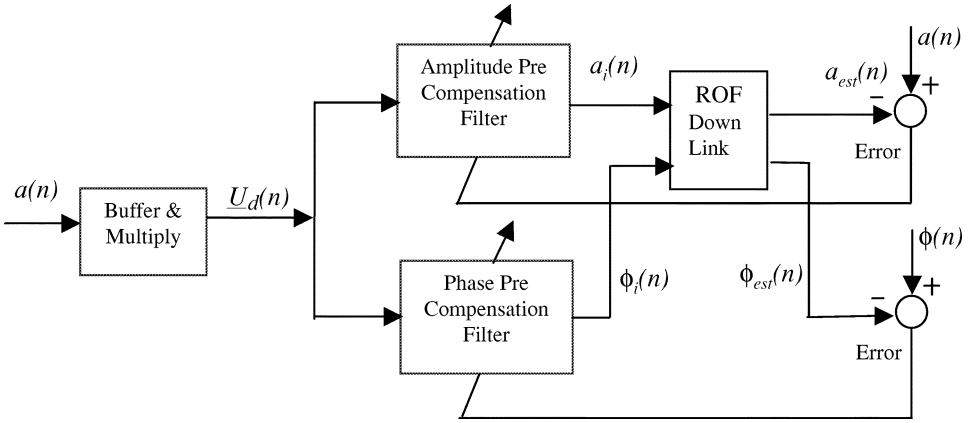

Fig. 4. Training arrangement for the pre-compensation filter.

$d(n)$ and the estimated output $d_{\text{est}}(n)$ is minimized in a mean-squared sense as in

$$\min_{\mathbf{w}(n)} E[e^2(n)]. \tag{6}$$

The recursive least squares (RLS) algorithm is used here, due to its fast convergence properties with correlated inputs, to recursively solve the problem. Adjacent samples are correlated here since the input amplitude changes are much slower than the sampling rate. According to the RLS algorithm, the exponentially weighted cost function in (7) must be minimized, where λ is a *forgetting factor* $(0.95 < \lambda < 1)$ that accounts for nonstationary environments

$$J(n) = \sum_{k=1}^{n} \lambda^{n-k}[d(n) - d_{\text{est}}(n)]^2. \tag{7}$$

The optimal vector $\mathbf{w}(n)$, which minimizes $J(n)$, is given by

$$\mathbf{w}(n) = \mathbf{R}^{-1}(n)\Gamma(n). \tag{8}$$

Here, $\mathbf{R}(n)$ is the autocorrelation matrix of the input vector $\mathbf{u}(n)$ and is defined

$$\mathbf{R}(n) = \sum_{k=1}^{n} \lambda^{n-k}\mathbf{u}(n)\mathbf{u}^T(n). \tag{9}$$

In (8) and (9) the vector $\mathbf{\Gamma}(n)$ is the cross correlation vector between the input vector $\mathbf{u}(n)$ and the desired response $d(n)$ and is defined in (10). The RLS algorithm implements the expression in (8) recursively, as summarized in [18]

$$\mathbf{\Gamma}(n) = \sum_{k=1}^{n} \lambda^{n-k}\mathbf{u}(n)d(n). \tag{10}$$

B. ROF Link Nonlinearity Compensation

The post-compensation arrangement is shown Fig. 3 and the pre-compensation arrangement is shown in Fig. 4. Without loss of generality, we assume that, except for the ROF link, all other elements from the portable to the base station are ideal. Under this assumption, the distortion of the received sequence is only due to the ROF link. Now, consider a training sequence, $d(n)$, defined in (11) with known amplitude $a(n)$ and phase $\phi(n)$

$$d(n) = a(n)e^{j\phi(n)}. \tag{11}$$

In the uplink transmission $d(n)$ is transmitted from the RAP. Thus, after transmission through the ROF link, the received symbol $d_r(n)$ has distorted amplitude $a_r(n)$ and a phase error $\theta_r(n)$, given by (12), due to the ROF link

$$d_r(n) = a_r(n)e^{j(\phi(n)+\theta_r(n))}. \tag{12}$$

In the downlink transmission, $d(n)$ is transmitted from the central base station. After pre-distortion the intermediate symbol $d_i(n)$ has amplitude $a_i(n)$ and a phase shift $\theta_i(n)$ at the input of the ROF link

$$d_1(n) = a_1(n)e^{j(\phi(n)+\theta_1(n))}. \tag{13}$$

In both links, the output of the combined system (filter plus link) is $d_{\rm est}(n)$, with amplitude $a_{\rm est}(n)$ and phase shift $\theta_{\rm est}(n)$

$$d_{\rm est}(n) = a_{\rm est}(n)e^{j(\phi(n)+\theta_{\rm est}(n))}. \tag{14}$$

This $d_{\rm est}(n)$ has to be compared with $d(n)$ during training. In the uplink, $d_{\rm est}(n)$ is available at the central base station and can be compared with a stored copy of the desired signal $d(n)$. However, in the downlink, the estimate $d_{\rm est}(n)$ is available only at the RAP and has to be transmitted back to the base station. This has some practical difficulties that are discussed in Section VI. In any case, since the filters inverse model the link, after convergence $d_{\rm est}(n)$ will closely resemble $d(n)$ and the error $e(n)$ will approach zero. That means $\theta_{\rm est}(n)$ will approach zero and $a_{\rm est}(n)$ will approach $a(n)$. Define the estimated phase as $\phi_{\rm est}(n) = \phi(n) + \theta_{\rm est}(n)$ then, $\phi_{\rm est}(n)$ will approach $\phi(n)$.

The RF powers corresponding to the symbols in (11) and (12), assuming a one-Ohm resistance at each location, are given by

$$p(n) = \frac{a^2(n)}{2} \tag{15}$$

$$p_r(n) = \frac{a_r^2(n)}{2}. \tag{16}$$

The adaptive filters have to be designed to apply compensation to the base band symbols as a function of their RF power. The use of two separate filters for amplitude and phase compensation yielded better results because the amplitude and phase nonlinearities are independent of each other. The two filters have exactly the same architecture except that, for amplitude compensation, the system output is compared with $a(n)$ while for phase compensation it is compared with $\phi(n)$. This is true in both up and down link transmissions. These schemes are shown in Figs. 3 and 4, respectively.

Strictly speaking, memory of the nonlinear system should be considered. However, memory of the ROF link is negligible up to several Mb/s because of its enormous bandwidth [19]. Thus, for the data rate considered, a memoryless filter was used. In that case, M is set equal to zero and the expression in (4) simplifies into a polynomial equation. Define the tap input vector $\mathbf{u}_r(n)$ to the post-compensation filter as

$$\mathbf{u}_r(n) = \begin{bmatrix} 1 & p_r(n) & p_r^2(n) & \dots & p_r^N(n) \end{bmatrix}^T. \tag{17}$$

The input vector $\mathbf{u}_r(n)$ is the same for both amplitude and phase filters, however, their orders are not necessarily the same. This input vector is multiplied by the weight vector $\mathbf{w}_r(n)$ of the amplitude post-compensation filter to obtain the output amplitude $a_{\rm est}(n)$ and is multiplied by the weight vector $\mathbf{w}_\phi(n)$ of the phase post-compensation filter to obtain the output phase $\phi_{\rm est}(n)$, respectively, as in

$$a_{\rm est}(n) = \mathbf{w}_a(n)\mathbf{u}^T(n) \tag{18}$$

$$\varphi_{\rm est}(n) = \mathbf{w}_\phi(n)\mathbf{u}^T(n). \tag{19}$$

Thus, the outputs of the filters are polynomial functions of the input RF power with the appropriate weights. The estimated amplitude $a_{\rm est}(n)$ and phase $\phi_{\rm est}(n)$ are then compared with stored copies of $a(n)$ and $\phi(n)$, respectively, to create error terms as shown in Fig. 3.

In the downlink, the tap input vector, $\mathbf{u}_d(n)$, to the pre-compensation filter is defined as

$$\mathbf{u}_d(n) = \begin{bmatrix} 1 & p(n) & p^2(n) & \dots & p^N(n) \end{bmatrix}^T. \tag{20}$$

In contrast to the uplink, the vector $\mathbf{u}_d(n)$ consists of the RF power of the original symbol $d(n)$, which eases pre-compensation. This input vector is multiplied by the weight vectors of amplitude and phase pre-compensation filters to obtain the outputs $a_i(n)$ and $\phi_i(n)$, respectively, as shown in Fig. 4. Note that now the intermediate amplitude $a_i(n)$ and phase $\phi_i(n)$ are going through the ROF link to obtain $a_{\rm est}(n)$ and $\phi_{\rm est}(n)$ before comparison.

V. Measurements and Simulation

Experimental measurements were taken on a ROF link that consists of a 1310-nm InGaAsP-distributed feedback (DFB) laser, 2.2-km 9/125 single-mode fiber, and a positive-intrinsic-negative (PIN) diode receiver. The optical link loss is compensated with a high-gain receiver amplifier so that the overall gain is approximately one. The link is reactively matched to have a flat frequency response from 1.7 to 2.2 GHz. The amplitude and phase responses of this link were measured at 1.8 GHz using a vector modulation analyzer and are shown in Fig. 2. The responses are consistent within the pass band.

The experimental data was used to run the simulation in Simulink environment running in Matlab platform. Vector-modulated symbols were transmitted via the simulated ROF link to train the filters as shown in Figs. 3 and 4; 2000 iterations were run each time. The forgetting factor λ was set to unity assuming a stationary environment. The measurements were taken up to 2.5 mW and the simulation was run by varying $p(n)$ from zero to a maximum value $p_{\max}$ ($<$2.5 mW) because the convergence was a function of $p_{\max}$. We refer to this range as the dynamic range (DR). Furthermore, from Fig. 2, the output power saturates softly until 0.74 mW, which is attained when the input power is about 1.2 mW. After this point, the output power does not increase with increase in the input. We refer to this $p_{\max}$ input as the clipping limit. The actual dynamic range is normalized with respect to this $p_{\max}$ so as to generalize the results.

A. Amplitude Post-Compensation

Convergence heavily depends on the dynamic range (DR) and filter order N. To study this effect, the simulation was run with different filter lengths N and dynamic range, DR. The minimum mean squared error (MMSE), which is an indication of convergence, is plotted versus N in Fig. 5. The MMSE achieved a steady state within the first 400–500 symbols. Fig. 5 shows that the lowest MMSE is achieved when the input dynamic range is within 83.3% of the clipping limit, which corresponds to a

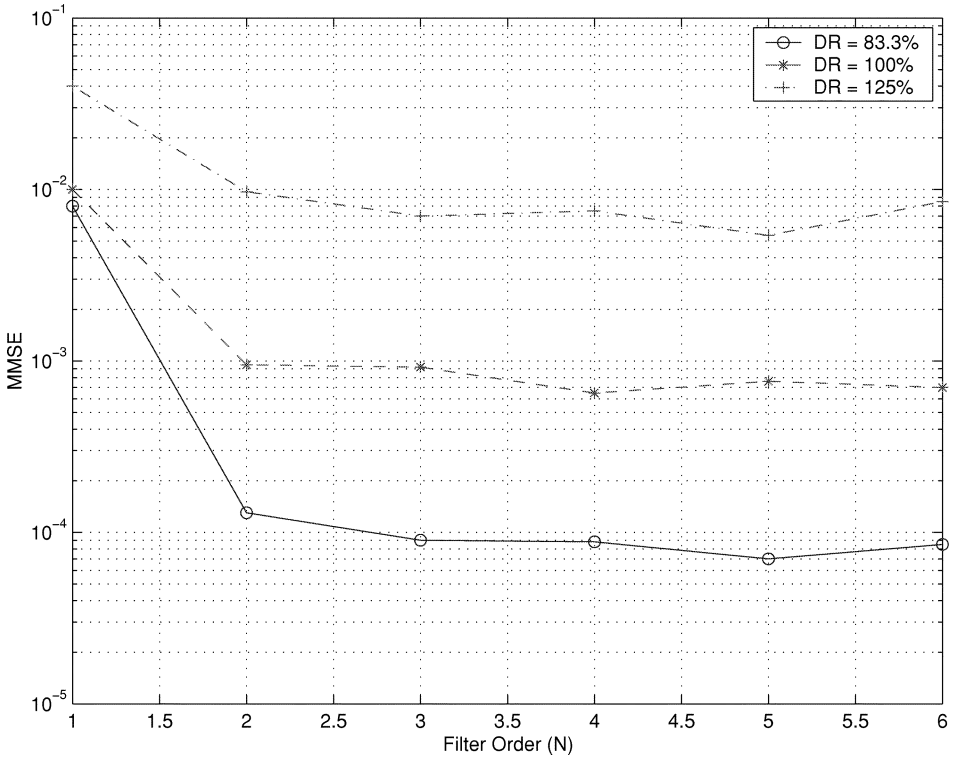

Fig. 5. Effect of the dynamic range.

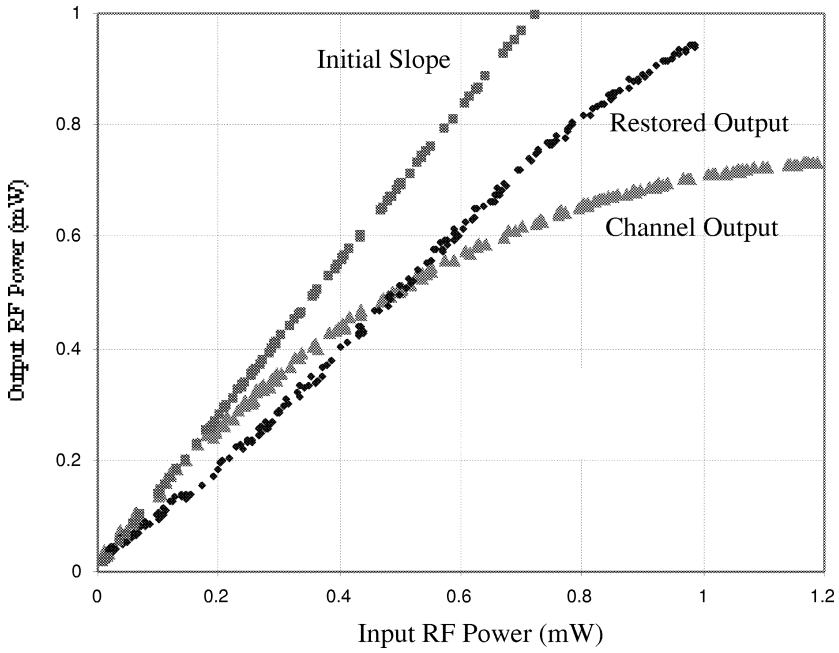

Fig. 6. Amplitude post-compensation with a second-order filter.

16.7% power backoff. In this case, a second-order filter is adequate. Higher order filter terms only marginally reduce the MMSE, with increased complexity.

The linearized amplitude responses with a second-order filter as well as the uncompensated channel output are shown in Fig. 6. The channel output has an initial slope of about 1.38, which is shown by an asymptotic straight line. However, it starts to saturate rapidly, attaining a unity gain at 0.5 mW and fully saturating at 1.2 mW. On the other hand, the restored output is almost linear up to 0.9 mW and shows a small deviation after that.

Compression of a curve can be defined as the decrement in its slope from the initial value. The compression of both the channel output and the restored output are shown in Fig. 7. The channel output has its 1-dB compression point at 0.4 mW and the compression is as high as 3 dB at 1.0 mW. However, the compression of the restored output remains within 0.5 dB for the entire dynamic range.

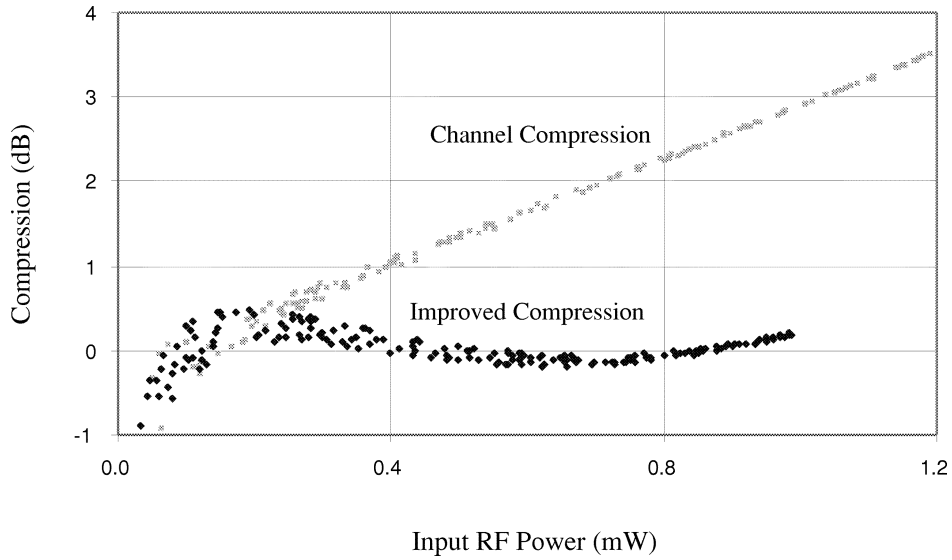

Fig. 7. Compression from the initial slope.

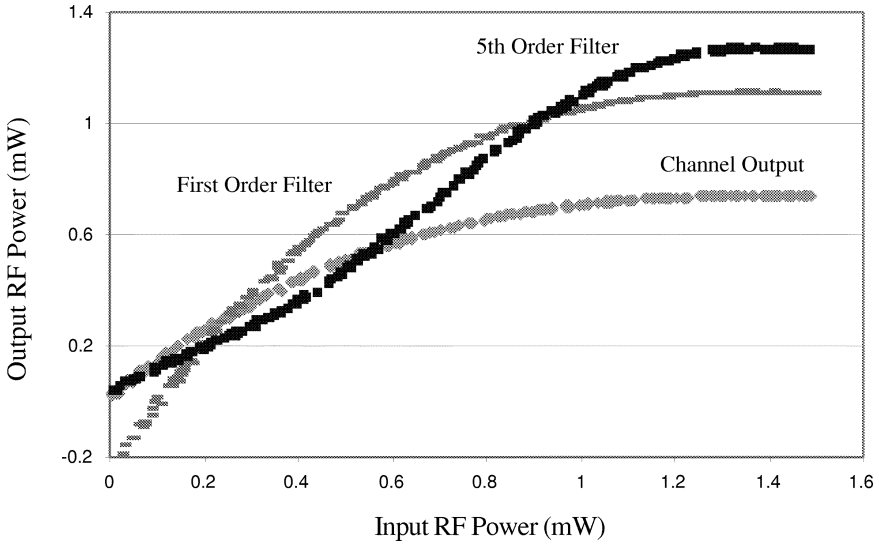

Fig. 8. Amplitude post-compensation with different filter orders.

When the dynamic range is large (83.3% of the clipping limit), even a fifth-order filter is unable to provide good linearity as shown in Fig. 8. Observe the fluctuation in the slope even at lower input levels level. The major reason for this phenomenon is because, close to saturation, the correlation between the filter input power and the estimated output rapidly decreases. Nevertheless, the RLS algorithm struggles to achieve some weights for the whole dynamic range. This may be slightly improved by selecting closer sampling points, especially near the saturation region.

B. Phase Post-Compensation

It was also found that a third-order filter is adequate for phase compensation. The error between the original phase and the restored phase is within ± 0.1 radians, up to 2 mW or 167% of the clipping limits (Fig. 9). This is adequate for most practical applications and can be further reduced if a lower dynamic range is used during training. However, when the input amplitude is high the error increases. This is because when the input amplitude is high (in the clipping region) there is less correlation between input and output power, while the filter uses the distorted output power $p_r(n)$ to estimate the phase distortion. However, we note that when the amplitude compensation filter is first deployed to restore the amplitude from $p_r(n)$ and the restored amplitude is then used to create the input vector to the phase compensation filter (refer to the final arrangement in Fig. 11), the performance is much improved, with a phase error within ± 0.03 radians. This error is also shown in Fig. 9. However, the useful dynamic range is now reduced to 1 mW (or 83.3%) by the limitation of the amplitude compensation filter.

C. Pre-Compensation

For amplitude pre-compensation, the optimum filter order is determined by running the filter with different orders within different dynamic ranges as before. It was found that at least a third-order filter is needed for adequate compensation.

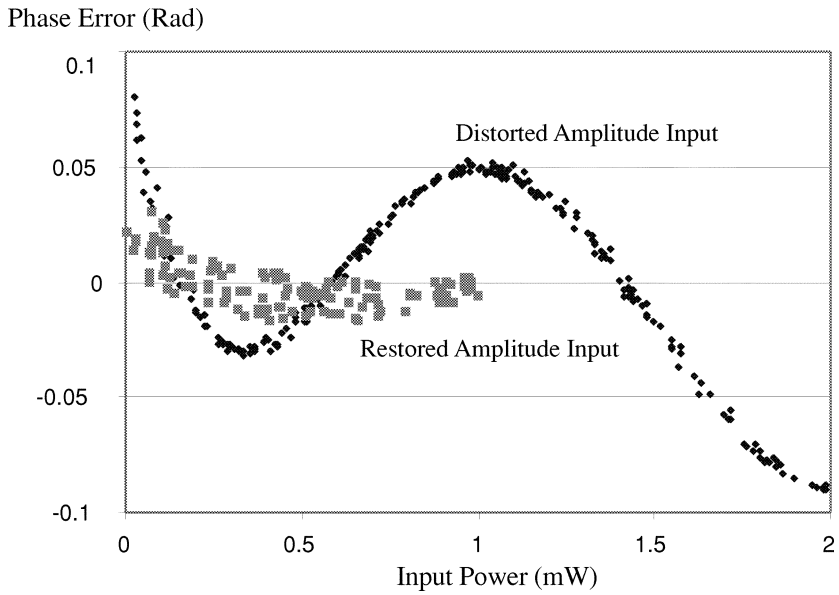

Fig. 9. Phase post-compensation using a third-order filter.

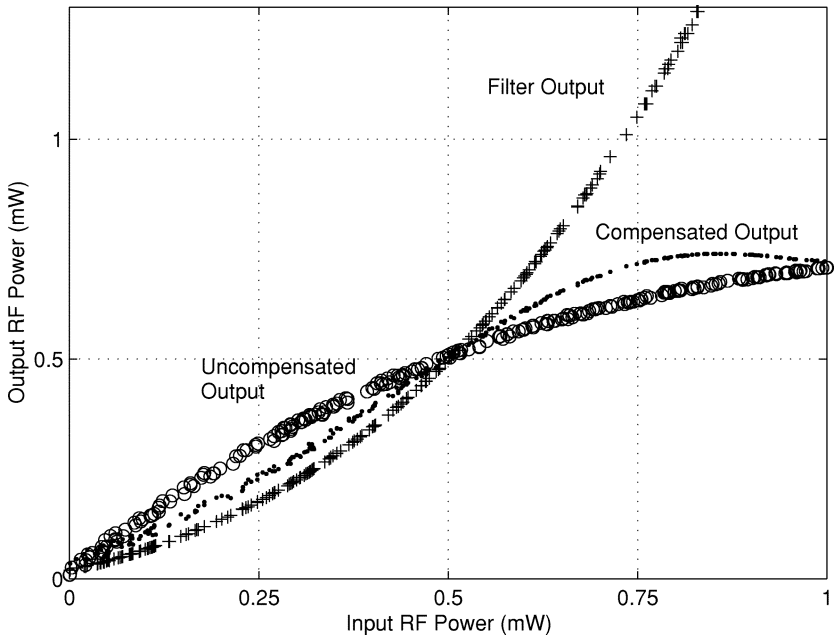

Fig. 10. Amplitude pre-distortion using a third-order filter.

However, a 42% power backoff is now required to achieve good linearity compared to 16.7% for post compensation. Fig. 10 shows the uncompensated, the compensated and the filter output powers as a function of the system input power. It can be seen that to overcome saturation, output power exponentially increases with the input power $p(n)$. This exceeds the specified maximum power of the laser much before the clipping limit. Thus, significant power backoff is required for pre-compensation to protect the laser even during training. However, with this much backoff, the linearity achieved is as good as that of the post-compensation.

Phase pre-compensation works well, giving an error within ± 0.01 radians with just a second-order filter. Furthermore, phase is easily adjusted without any concern on the power specifications of the laser and the maximum phase shift is within 180°. Moreover, the variation in the phase response decreases with the RF power in ROF links. Phase pre-compensation is therefore the easiest to accomplish, even at higher power levels. The reader is referred to [13] for more discussion and constellation plots with phase pre-distortion.

VI. Conclusion and Discussion

In this paper, an asymmetric nonlinearity compensation scheme, based upon higher order adaptive filters, is described for radio-over-fiber links. Although the discussion is focused on directly modulated links, it is readily extendable to other types of optical modulation schemes. The results of pre- and post-compensation are summarized in Table I. Final arrangement of the filters is shown in Fig. 11. This adaptive modeling

TABLE I
SUMMARY OF ASYMMETRIC MEMORYLESS COMPENSATION SCHEMES

Compensation Type	Amplitude	Phase
Post-Compensation	Works well with a small back off	Works well when the restored amplitude is used for estimation
Pre-Compensation	Considerable back off is required due to the power handling capability of the laser	Works well since the distortion is a function of the input power and the filter uses the same input power for estimation

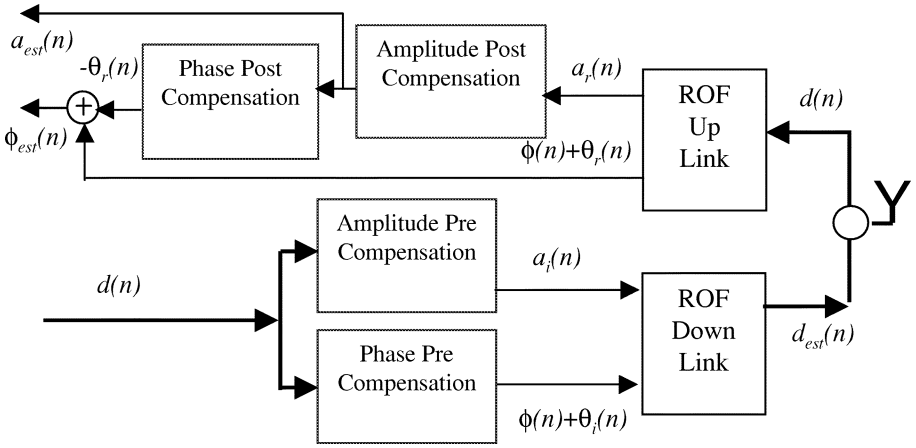

Fig. 11. Final asymmetric compensation arrangement.

approach is a function of input–output characteristics only and is independent of explicit knowledge of the individual optical link parameters such as optical wavelength, fiber length and exact characteristics of the laser. However, the order of the filters must be adequate for a given dynamic range.

Electrical-domain signal processing techniques are seldom used in fiber-optic links since the degradations are in a different domain. However, the radio-over-fiber is a unique application where all the information is carried by base band symbols and we have access to these symbols at both ends of the link. This enables modeling of the entire ROF link at base band and the application of base-band signal processing techniques.

In this work, we have justifiably assumed memoryless mild nonlinearity so that simple polynomial filters are used. However, when this is not the case, more advanced compensation schemes need to be investigated. Impairments of the other elements, especially the wireless channel must also be considered for a complete solution. Another issue is training the pre-compensation filter. This requires the estimated outputs to be transmitted back to the central base station. This is a challenging task because of the distortion in the ROF uplink. One way of approaching this problem is to first accomplish the uplink compensation before the downlink compensation. These need to be coordinated with higher layer protocols. A constant noise power was used during simulation. Nevertheless, a nonlinear increment in the ROF link noise was observed when the signal power is high. This needs further investigation.

ACKNOWLEDGMENT

The authors would like to thank Dr. B. Davies, TRLabs, Calgary, Alberta, Canada, for useful discussions on analog optical links.

REFERENCES

[1] W. I. Way, "Optical fiber based microcellular systems: An overview," *IEICE Trans. Commun.*, vol. E76-B, no. 9, pp. 1091–1102, Sept. 1993.
[2] C. Cox III, E. Ackerman, R. Helkey, and G. E. Betts, "Techniques and performance of intensity-modulation direct detection analog optical links," *IEEE Trans. Microwave Theory Tech.*, vol. 45, Aug. 1997.
[3] R. S. Tucker, "High speed modulation of semiconductor lasers," *IEEE J. Lightwave Technol.*, vol. LT-3, pp. 1180–1192, Dec. 1985.
[4] P. Raziq and M. Nagakawa, "Semiconductor laser's nonlinearity compensation for DS-CDMA optical transmission system by post nonlinearity recovery block," *IEICE Trans. Commun.*, vol. E-79 B, no. 3, Mar. 1996.
[5] L. S. Fock and R. S. Tucker, "Simultaneous reduction of intensity noise and distortion in semiconductor laser by feed forward compensation," *Electron. Lett.*, vol. 27, no. 14, pp. 1297–1298, July 1991.
[6] H. Gysel and M. Ramachandran, "Electrical pre-distortion to compensate for combined effect laser chirp and fiber dispersion," *Electron. Lett.*, vol. 27, no. 5, Feb. 1991.
[7] P. Vankwikelberge *et al.*, "Analysis of the carrier induced FM response of the DFB lasers," *IEEE J. Quantum Electron*, vol. 25, pp. 2239–2254, Nov. 1989.
[8] F. Cheng, P. Lemson, J. H. Reed, and I. Jacobs, "A dynamic range enhancement technique for fiber optic microcell radio systems," in *Proc. Vehicular Technology Conf. (VTC) 45*, Chicago, IL, July 1995, pp. 774–778.
[9] D. M. Cutrer, J. B. Georges, T. H. Le, and K. Y. Lau, "Dynamic range requirements for optical transmitters in fiber fed microcellular networks," *IEEE Photon. Technol. Lett.*, vol. 7, pp. 564–566, May 1995.

[10] W. Huang, E. A. Sourour, and M. Nakagawa, "Cancellation technique used for DS-CDMA signal in nonlinear optical link," *IEICE Trans. Fundamentals Electron.*, vol. E80, no. A. 9, Sept. 1997.
[11] W. I. Way, "Subcarrier multiplexed lightwave system design considerations for subscriber loop applications," *IEEE J. Lightwave Technol.*, vol. 7, pp. 1806–1818, Nov. 1989.
[12] W. E. Stephens and T. R. Joseph, "System characteristics of direct modulated and externally modulated RF fiber optic links," *IEEE J. Lightwave Technol.*, vol. LT-5, pp. 380–387, Mar. 1987.
[13] X. N. Fernando and A. Sesay, "Higher order adaptive filter based pre-distortion for nonlinear distortion compensation of radio over fiber links," in *Proc. Int. Conf. Communications 2000*, New Orleans, LA, June 2000, paper S08P1.
[14] ——, "Nonlinear distortion compensation of microwave fiber optic links with asymmetric adaptive filters," in *Proc. 2000 Int. Microwave Symp. Dig.*, Boston, MA, June 2000, Session THIF-11.
[15] *A System Designer's Guide to RF and Microwave Fiber Optics*, Ortel Corp., Alhambra, CA, 1997.
[16] W. Bosch and G. Gatti, "Measurements and simulation of memory effects on pre-distortion linearizers," *IEEE Trans. Microwave Theory Tech.*, vol. 37, pp. 1885–1890, Dec. 1989.
[17] A. M. Saleh, "Frequency-independent and- frequency-dependent nonlinear models of TWT amplifiers," *IEEE Trans. Commun.*, vol. COM-29, pp. 1715–1720, Nov. 1981.
[18] S. Haykin, *Adaptive Filter Theory*, 3rd ed. Englewood Cliffs, NJ: Prentice-Hall, 1996, p. 566.
[19] G. Einarsson, *Principles of Lightwave Communications*. West Sussex, U.K.: Wiley, 1995.

Xavier N. Fernando (S'97–M'01) received the B.Sc.Eng. degree (first class, with honors) in electrical and electronic engineering from the University of Peradeniya, Sri Lanka, in 1992, the Master's degree in telecommunications at the Asian Institute of Technology (AIT), Bangkok, Thailand, in 1994 (under a Finnish International Development Agency (FINNIDA) Scholarship), and the Ph.D. degree from the University of Calgary, Calgary, Canada, in the area of optical-wireless communications in 2001.

Currently, he is an Assistant Professor at Ryerson University, Toronto, Canada. He was an R&D Engineer for AT&T Thailand from 1994 to 1997. He has a patent pending innovation and is the first author of several journal articles, conference papers, and technical reports. His research interest includes wireless networks, optical techniques for wireless access, and adaptive signals and systems.

Dr. Fernando was the the recipient of the Best Student Paper Award at the Canadian Conference on Electrical and Computer Engineering (CCECE'01) 2001. He was awarded TRLabs, NSERC, and Alberta Informatics Circle of Research Excellence (ICORE) Scholarships.

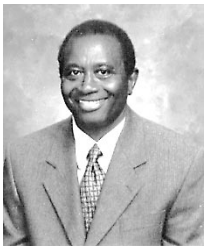

Abu B. Sesay (SM'01) received the Ph.D. degree in electrical engineering from McMaster University, Hamilton, ON, Canada, in 1988.

He worked on various ITU projects from 1979 to 1984. In 1989, he joined the University of Calgary where he is now a Full Professor and Associate Head. He has been involved with TRLabs since 1989, where he is now a TRLabs Adjuct Scientist. His current research activities include space-time coding, MC-CDMA, multi-user detection, equalization, optical fiber/wireless communications, and adaptive signal processing.

Dr. Sesay is the recipient of the IEEE 1996 Neal Shepherd Memorial Best Propagation Paper Award. He is also the recipient of the Departmental Research Excellence Award for 2001. His students have received three IEEE conference best paper awards.